Journal of Analytical Sciences, Methods and Instrumentation, 2014, 4, 19-26
Published Online March 2014 in SciRes. http://www.scirp.org/journal/jasmi
http://dx.doi.org/10.4236/jasmi.2014.41003

Scientific Research

Ultrafast Laser Energy Density and Retinal Absorption Cross-Section Determination by Saturable Absorption Measurements

Alfons Penzkofer[1*], Meike Luck[2], Tilo Mathes[2,3], Peter Hegemann[2]

[1]Faculty of Physics, University of Regensburg, Regensburg, Germany
[2]Institute of Biology/Experimental Biophysics, Humboldt University to Berlin, Berlin, Germany
[3]Department of Exact Sciences/Biophysics, Vrije Universiteit, Amsterdam, The Netherlands
Email: [*] alfons.penzkofer@physik.uni-regensburg.de

Received 7 January 2014; revised 7 February 2014; accepted 15 February 2014

Abstract

Laser pulse nonlinear transmission measurements through saturable absorbers of known absorption parameters allow the measurement of their energy density. On the other hand, nonlinear transmission measurements of laser pulses of known energy density through absorbing media allow their absorption parameter determination. The peak energy density w_{0P} of second harmonic pulses of a mode-locked titanium sapphire laser at wavelength λ_P = 400 nm is determined by nonlinear energy transmission measurement T_E through the dye ADS084BE (1,4-bis(9-ethyl-3-carbazovinylene)-2-methoxy-5-(2'-ethyl-hexyloxy)-benzene) in tetrahydrofuran. $T_E(w_{0P})$ calibration curves are calculated for laser pulse peak energy density reading w_{0P} from measured pulse energy transmissions T_E. The ground-state absorption cross-section σ_P and the excited-state absorption cross-section σ_{ex} at λ_P, and the number density N_0 of the retinal Schiff base isoform RetA in pH 7.4 buffer of the blue-light adapted recombinant rhodopsin fragment of the histidine kinase rhodopsin HKR1 from *Chlamydomonas reinhardtii* were determined by picosecond titanium sapphire second harmonic laser pulse energy transmission measurement T_E through RetA as a function of laser input peak energy density w_{0P}. The complete absorption cross-section spectrum $\sigma(\lambda)$ of RetA was obtained by absorption coefficient spectrum measurement $\alpha(\lambda)$ and normalization to the determined absorption cross-section σ_P at λ_P [$\sigma(\lambda) = \alpha(\lambda)\sigma_P/\alpha_P$].

Keywords

Laser Pulse Peak Energy Density Determination; Ground-State Absorption Cross-Section Determination; Excited-State Absorption Cross-Section Determination; Saturable Absorption; ADS084BE Dye; Histidine Kinase Rhodopsin HKR1; Retinal Schiff Base RetA Cofactor; Number Density Determination

[*]Corresponding author.

How to cite this paper: Penzkofer, A., Luck, M., Mathes, T. and Hegemann, P. (2014) Ultrafast Laser Energy Density and Retinal Absorption Cross-Section Determination by Saturable Absorption Measurements. *Journal of Analytical Sciences, Methods and Instrumentation*, **4**, 19-26. http://dx.doi.org/10.4236/jasmi.2014.41003

1. Introduction

Saturable absorption measurements may be used to determine the peak intensity or peak energy density of laser pulses [1]. For peak intensity detection saturable absorbers with ground-state absorption recovery time τ_A short compared to the laser pulse duration Δt_P are appropriate. For peak energy density detection saturable absorbers (dyes) with fluorescence lifetime τ_F long compared to the laser pulse duration are suited. The fast saturable absorber technique was applied to determine the peak intensity of picosecond Nd:glass lasers at 1054 nm [2] (saturable absorber: mode-locking dye A9860 in 1,2-dichloroethane) and ruby lasers [3] (saturable absorber DDI in methanol). The slow saturable absorber technique was applied to measure the peak pulse energy density of Nd:glass lasers (fundamental: BDN I in 1,2-dichloroethane, second harmonic: rhodamine 6G in ethanol, third harmonic: dimethyl POPOP in cyclohexane, fourth harmonic: 9,10-dimethylanthracene in cyclohexane) and ruby lasers (fundamental: DDI in glycerol, second harmonic: dimethyl POPOP in cyclohexane) [4].

Here the peak energy density w_{0P} of picosecond second harmonic pulses of a mode-locked Ti:sapphire laser (wavelength λ_P = 400 nm, pulse duration $\Delta t_P \approx 5$ ps) was measured using the dicarbazavinylene-MEH-benzene dye ADS084BE (from American Dye Source Inc., Quebec, Canada) in tetrahydrofuran (THF). The structural formula of ADS084BE is shown in **Figure 1**. Its absorption cross-section spectrum is shown in **Figure 2** (from [5]). Further relevant parameters of ADS084BE required for the calculation of the energy transmission T_E versus input pump pulse peak energy density w_{0P} are collected in **Table 1** (from [5]). Two curves of $T_E(w_{0P})$ were determined for two different small-signal transmissions T_0 of ADS084BE in THF.

The energy transmission, $T_E(w_{0P})$, of picosecond titanium sapphire second harmonic laser pulses (λ_P = 400 nm, $\Delta t_P \approx 5$ ps) through retinal Schiff base RetA in pH 7.4 HEPES/DDM buffer (20 mM 2-[4-(2-hydroxyethyl)-1-piperazin-1-yl]ethansulfonic acid, 100 mM NaCl, 10 vol-% glycerol containing 0.03 m/v-% DDM (n-dodecyl-ß-D-maltoside)) of the blue-light adapted rhodopsin fragment of the histidine kinase rhodopsin HKR1 from *Chlamydomonas reinhardtii* [6] was measured to determine its ground-state absorption cross-section σ_P, excited state absorption cross-section σ_{ex}, and number density N_0 (concentration $C_0 = N_0/N_A$ where N_A is the Avogadro constant). Knowing the absolute absorption cross-section of RetA at the fixed wavelength λ_P, its whole absorption cross-section spectrum is obtained by measuring the absorption coefficient spectrum $\alpha(\lambda)$ with a conventional spectrophotometer and calculation of the absorption cross-section spectrum by the relation $\sigma(\lambda) = \alpha(\lambda)\sigma(\lambda_P)/\alpha(\lambda_P)$ since the number density of RetA is given by $N_0 = \alpha(\lambda_P)/\sigma(\lambda_P)$. The absorp-

Table 1. Parameters of reference dye ADS084BE in THF and of blue-light adapted cofactor RetA of HKR1 in HEPES/DDM pH 7.4 buffer used for saturable absorption calculations.

Parameter	ADS084BE	RetA	Comments
M_m (g·mol^{-1})	674.91	34520[a)]	
η (Pa s)	4.8×10^{-4}	0.001	
ρ (g cm^{-3})	1.4	1.4	Assumed [12]
V_m (nm^3)	0.767	40.9 [a)]	$V_m = M_m/(N_A\rho)$
ϑ (K)	293	293	Experimental
λ_P (nm)	400	400	Experimental
Δt_P (ps)	5	5	Experimental
σ_P (cm^2)	2.263×10^{-16} [5]	Best fit: $(2 \pm 0.2) \times 10^{-16}$	
σ_{ex} (cm^2)	Best fit: 4.35×10^{-17}	Best fit: $(1.29 \pm 0.32) \times 10^{-16}$	
τ_F (s)	1.5×10^{-9} [5]	3.64×10^{-11} [b)] [7]	
τ_{FC} (s)	5×10^{-13}	5×10^{-13}	Assumed [13]
τ_{ex} (s)	6×10^{-15}	6×10^{-15}	Assumed [14]
τ_{or} (s)	9.1×10^{-11}	9.1×10^{-8}	$\tau_{or} = \eta V_m/(k_B\vartheta)$ [9]

a: of HKR1 rhodosin. b: mean excited-state lifetime $\bar{\tau}_{em}$ [7]. Abbreviations: M_m: molar mass. η: viscosity. ρ: mass density. V_m: molecule volume. ϑ: temperature. k_B: Boltzmann constant. λ_P: pump laser wavelength. Δt_p: pump laser pulse duration (FWHM). σ_p: ground-state absorption cross-section at pump laser wavelength. σ_{ex}: excited-state absorption cross-section at pump laser wavelength. τ_F: fluorescence lifetime. τ_{FC}: Franck-Condon relaxation time. τ_{ex}: higher excited-state lifetime. τ_{or}: molecular reorientation time.

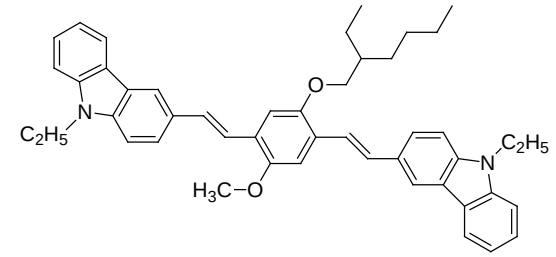

ADS084BE

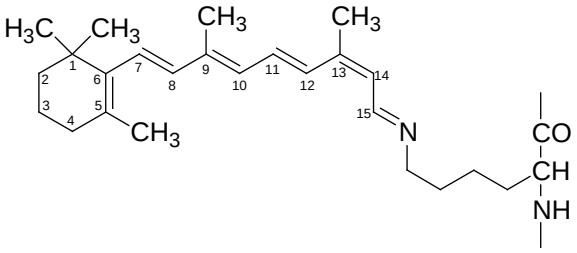

Deprotonated 13-*cis*,15-*anti* retinal Schiff base (RetA)

Figure 1. Structural formulae of ADS084BE (1,4-bis(9-ethyl-3-carbazovinylene)-2-methoxy-5-(2'-ethyl-hexyloxy)-benzene) and of retinal Schiff base isoform RetA with lysine residue coupled to rhodopsin.

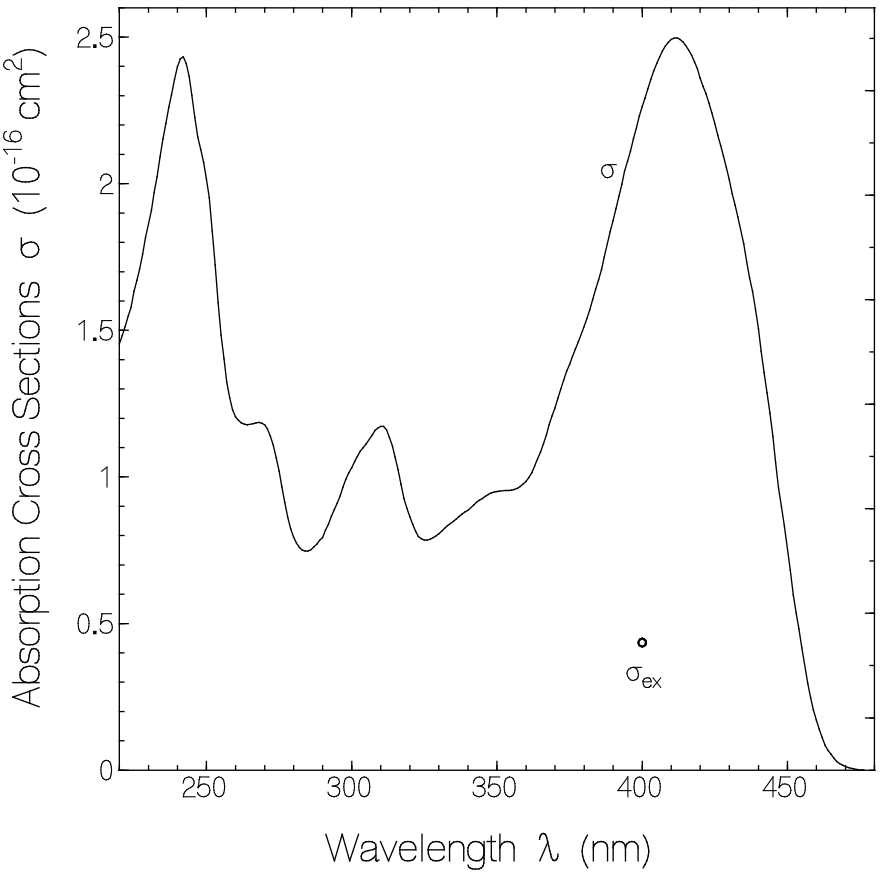

Figure 2. Absorption cross-section spectrum $\sigma(\lambda)$ of the absorber ADS084BE in THF. Circle: determined excited-state absorption cross-section σ_{ex} at λ_P = 400 nm.

tion cross-section spectrum of RetA was needed in the analysis of the photo-dynamics of HKR1 rhodopsin [7]. The structural formula of RetA is displayed in **Figure 1**. Relevant parameters of RetA cofactor in HKR1 rhodopsin for the absorption cross-section determination are collected in **Table 1** (from [6] [7]). Detailed information on the histidine kinase rhodopsin HKR1 from *Chlamydomonas reinhardtii* and its retinal Schiff base cofactor isoforms is found in [6] [7] and is not repeated here.

2. Experimental

The nonlinear energy transmission measurements were carried out with a mode-locked titanium sapphire laser oscillator–regenerative amplifier system (Hurricane from Spectra Physics). The experimental arrangement is sketched in **Figure 3**. The laser was operated at wavelength of 800 nm and pulse duration of ≈ 5 ps. The laser pulses were frequency doubled in a BBO crystal (phase-matched β-BaB_2O_4 crystal, from Eksma, crystal length: 3 mm). The fundamental laser light was blocked off (filter BF) and the second harmonic light passed to the sample S. The second harmonic laser pulse intensity at the sample position S was varied by working with and without lens L1 and with and without neutral density filters NF. The second harmonic laser pulse input pulse signal height $S_{P,in}$ was measured with the silicon photodiode PD1, and the transmitted pulse signal height $S_{P,out}$ was measured with the silicon photodiode PD2. The energy transmission T_E through the sample was obtained by the ratio $T_E = S_{P,out}/S_{P,in}$. The fused silica sample cell S of 2 mm path length was either filled with the dye ADS084BE in THF or the HKR1 rhodopsin in pH 7.4 HEPES/DDM buffer. The laser was operated in single-shot mode. It was fired every 10 seconds. Each energy transmission data point shown in **Figures 5** and **6** was obtained as an average over about 30 laser shots. The retinal cofactor in HKR1 rhodopsin was brought and kept in the RetA isoform by continuous sample irradiation at 470 nm with an intensity of I_{exc} = 1.5 mW cm^{-2} using a light emitting diode LED (from Thorlabs).

The absorption dynamics was simulated by using the absorber energy level scheme of **Figure 4**. Level 1 describes the S_0 ground-state. Its population number density is N_1. Level 2' is the excited Franck-Condon state in the S_1 band (population number density $N_{2'}$). Level 2 is the thermally relaxed state in the S_1 band (population number density N_2). Level 3 is a higher excited state in the singlet band S_n (population number density N_3). σ_P indicates the ground state absorption cross-section at the pump laser at wavelength λ_P (frequency $\nu_P = c_0/\lambda_P$ where c_0 is the vacuum light velocity). σ_{ex} denotes the excited absorption cross-section for S_1-S_n transition of the pump laser at the wavelength λ_P. τ_{FC} is the Franck-Condon relaxation time within the S_1 band. τ_F is the ground-state absorption recovery time constant (fluorescence lifetime). The picosecond pump pulse temporal and spatial intensity distribution is assumed to be Gaussian shaped ($I_P(t,r) = I_{0P}\exp(-t/\tau_P)\exp(-r^2/r_P^2)$, $w_P(r) = w_{0P}\exp(-r^2/r_P^2)$. The pump pulse energy transition through the sample is defined as

$$T_E = \frac{\int_0^\infty r\mathrm{d}r\int_{-\infty}^{\infty} I_P(t',r,\ell)\,\mathrm{d}t'}{\int_0^\infty r\mathrm{d}r\int_{-\infty}^{\infty} I_P(t',r,0)\,\mathrm{d}t'}, \tag{1}$$

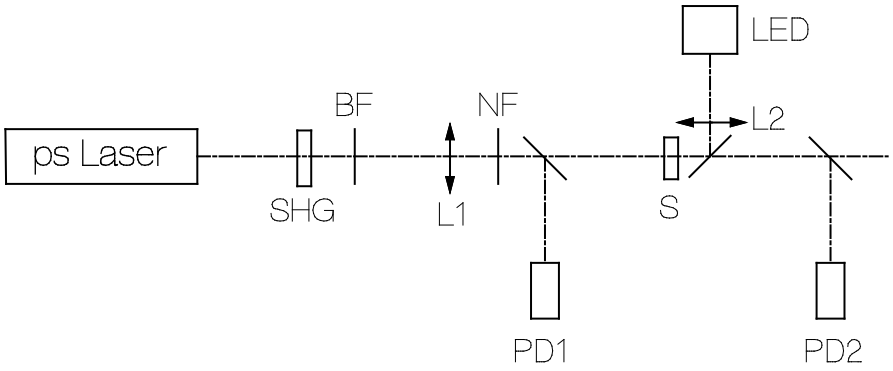

Figure 3. Schematic of experimental setup. ps Laser: mode-locked titanium sapphire oscillator–amplifier system. SHG: second harmonic generation. BF: fundamental laser blocking filter. NF: neutral density filter. L1, L2: lenses. S: sample. PD1, PD2: photo-detectors. LED: light emitting diode (LED 470 nm for blue-light adaptation of HKR1 rhodopsin).

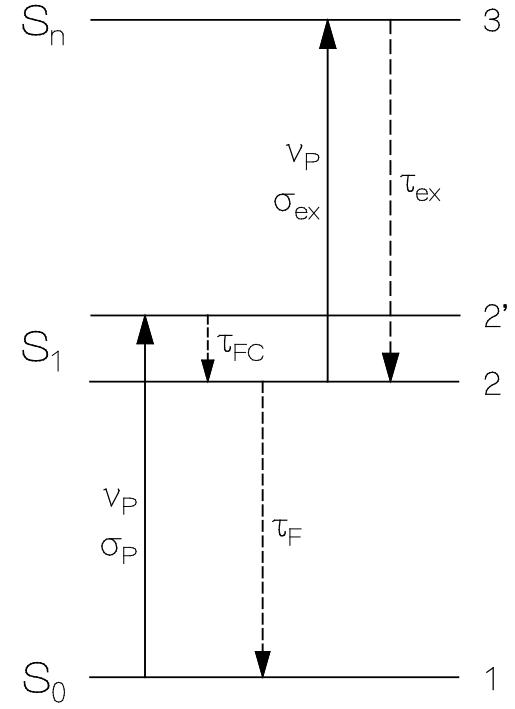

Figure 4. Energy level scheme. σ_P: ground-state absorption cross-section. σ_{ex}: excited-state absorption cross-section. τ_F: ground-state absorption recovery time. τ_{FC}: Franck-Condon relaxation time in first excited state. τ_{ex}: higher excited-state relaxation time. ν_P: pump laser frequency.

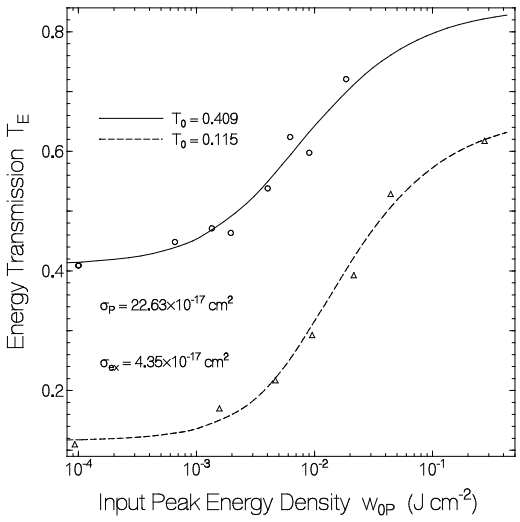

Figure 5. Energy transmission T_E versus input peak energy density w_{0P} through ADS084BE in THF. Circles and solid curve belong to sample length of ℓ = 2 mm and small signal transmission of T_0 = 0.409. Triangles and dashed curve belong to ℓ = 2 mm and T_0 = 0.115. Marks are experimental data. Curves are calculated. Applied parameters are collected in **Table 1**.

where ℓ is the sample length. The equation system for the level populations and the nonlinear pump pulse transmission through the sample is given in [8] and is not repeated here. It was solved numerically. The applied parameters in the calculations are collected in **Table 1**.

3. Results and Discussion

3.1. Calibration Curves for Pump Pulse Peak Energy Density Determination

In **Figure 5** two calculated energy transmission curves belonging to the dye ADS084BE in THF are shown for two different small-signal transmissions T_0 (ground-state absorption cross-section $\sigma_P = 2.236 \times 10^{-16}$ cm^2, sample length $\ell = 0.2$ cm). The dye parameters used in the calculations are listed in **Table 1**. The excited state absorption cross-section σ_{ex} of ADS084BE in THF was fitted to the experimental energy transmission results. For this purpose the T_E energy transmission data points were determined with the two photodiodes, PD1 and PD2, as a function of the photodiode signal height $S_{P,in}$ of PD1. $T_E(S_{P,in})$ was scaled to the input peak energy density abscissa w_{0P}. In the calculations σ_{ex} was varied until the best agreement between the shapes of experimental $T_E(S_{P,in})$ data and calculated $T_E(w_{0P})$ curves was obtained. The best fit was found for $\sigma_{ex} = 4.35 \times 10^{-17}$ cm^2.

After having the calculated calibration curves, the procedure of input pump pulse energy density determination is now the following: A sample of ADS094BE in THF is prepared with small-signal transmission of $T_0(\lambda_P) = 0.115$ or 0.409, then the energy transmission T_E is measured and w_{0P} is read from the relevant curve (w_{0P} abscissa to T_E ordinate).

3.2. Absorption Cross-Section and Number Density Determination of RetA

The energy transmission measurement results on a HKR1 rhodopsin sample with the retinal Schiff base cofactor in the RetA isoform (blue-light adapted) are displayed in **Figure 6**. The input peak energy densities for the data points were obtained by subsequent energy transmission measurements under the same experimental conditions on the dye ADS084BE. The solid curves in **Figure 6** are calculated energy transmission curves with the fixed parameters of **Table 1** for RetA and the varied parameters listed in the caption. Thereby the small signal transmission was set to the experimental value of $T_0 = 0.695$ and the limiting high pump pulse energy transmission of $T_e = 0.79$. A comparison of the calculated energy transmission curves with the experimental data gives $\sigma_P = (2.0 \pm 0.3) \times 10^{-16}$ cm^2 and $\sigma_{ex} = (1.29 \pm 0.2) \times 10^{-16}$ cm^2. The molar absorption coefficients [9] are $\varepsilon_P = \sigma_P N_A / [1000 \ln(10)] = (5.23 \pm 0.78) \times 10^4$ dm^3·mol^{-1}·cm^{-1} and $\varepsilon_{ex} = (3.37 \pm 0.5) \times 10^4$ dm^3·mol^{-1}·cm^{-1}. The RetA number density of the used sample is obtained by the relation $N_0 = -\ln(T_0)/(\sigma_P \ell)$ (sample length $\ell = 0.2$ cm) giving $N_0 = 9.1 \times 10^{15}$ cm^{-3} (concentration $C_0 = 1.51 \times 10^{-5}$ mol·dm^{-3}).

The complete absorption cross-section spectrum $\sigma(\lambda)$ of RetA is shown in **Figure 7**. It was obtained by measuring the transmission spectrum $T(\lambda)$ of RetA with a spectrophotometer (Cary 50 from Varian), transferring it to the absorption coefficient spectrum $\alpha(\lambda)$ by the relation $\alpha(\lambda) = -\ln[T(\lambda)]/\ell$ where ℓ is the sample length, and finally converting $\alpha(\lambda)$ to $\sigma(\lambda)$ by the relation $\sigma(\lambda) = \alpha(\lambda)\sigma_P / \alpha_P$.

4. Conclusions

The presented laser pulse peak energy density calibration curves for ADS084BE at λ_P= 400 nm were calculated for a pulse duration of $\Delta t_P = 5$ ps. But the energy transmission is nearly independent of the pulse duration as long as the laser pulse duration Δt_P is short compared to the absorption recovery time τ_F and the molecular reorientation time τ_{or}, and longer than the higher excited-state relaxation time τ_{ex}. Therefore they may be used with reasonable accuracy in the laser pulse duration range of 100 fs < Δt_P < 50 ps (see ADS084BE parameters of **Table 1**).

The described method of ground-state absorption cross-section σ_P, excited-state absorption cross-section σ_{ex}, and absorbing entity number density N_0 determination by $T_E(w_{0P})$ measurement and numerical $T_E(w_{0P})$ simulation of the excitation an relaxation dynamics for the level-system of **Figure 4** with known ground-state absorption recovery time $\tau_{F,}$, approximate molecular reorientation time τ_{or} and approximate higher excited-state recovery time τ_{ex} is generally applicable. It works for samples with $\sigma_P > \sigma_{ex}$ (saturable absorption [10]) and for samples with $\sigma_P < \sigma_{ex}$ (reverse saturable absorption [11]). It only fails for samples with $\sigma_P \approx \sigma_{ex}$ since in this case, the energy transmission is approximately independent of the pump pulse energy density ($T_E(w_{0P}) \approx T_0$).

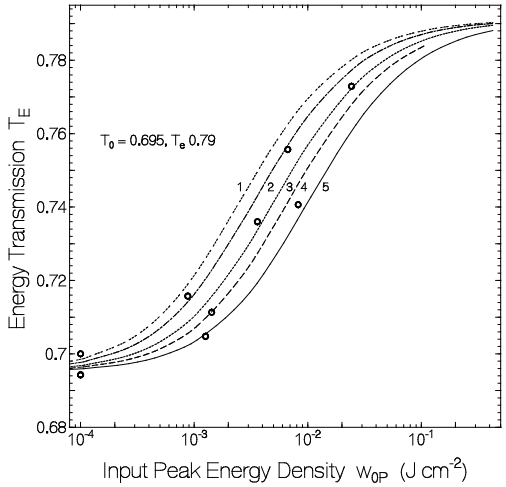

Figure 6. Energy transmission $T_E(w_{0P})$ of 5 ps laser pulses at 400 nm through sample of RetA in HEPES/DDM buffer at pH 7.4. Sample length ℓ = 2 mm. Small-signal transmission T_0 = 0.695. Data fit to limiting high input energy density transmission of $T_e = T_E(\infty) = 0.79$. The calculated curves belong to: (1) $\sigma_P = 4 \times 10^{-16}$ cm^2 and $\sigma_{ex} = 2.58 \times 10^{-16}$ cm^2 giving $N_0 = -\ln(T_0)/(\sigma_P \ell) = 4.55 \times 10^{15}$ cm^{-3}; (2) $\sigma_P = 3 \times 10^{-16}$ cm^2, $\sigma_{ex} = 1.94 \times 10^{-16}$ cm^2, $N_0 = 6.06 \times 10^{15}$ cm^{-3}; (3) $\sigma_P = 2 \times 10^{-16}$ cm^2, $\sigma_{ex} = 1.29 \times 10^{-16}$ cm^2, $N_0 = 9.1 \times 10^{15}$ cm^{-3}; (4) $\sigma_P = 1.5 \times 10^{-16}$ cm^2, $\sigma_{ex} = 9.69 \times 10^{-17}$ cm^2, $N_0 = 1.21 \times 10^{16}$ cm^{-3}; (5) $\sigma_P = 1 \times 10^{-16}$ cm^2, $\sigma_{ex} = 6.46 \times 10^{-17}$ cm^2, $N_0 = 1.82 \times 10^{16}$ cm^{-3}.

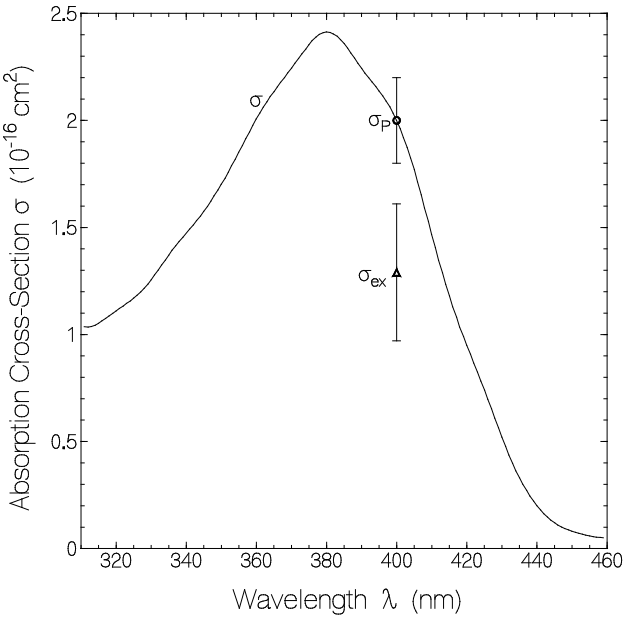

Figure 7. Absorption cross-section spectrum of RetA cofactor of HKR1 rhodopsin in pH 7.4 HEPES/DDM buffer. Experimental data points of σ_P (circle) and σ_{ex} (triangle) at λ_P = 400 nm are included.

Acknowledgements

The work was supported by the Deutsche Forschungsgemeinschaft (DFG, HE3824/19-1 and HE3824/29-1 to P. H.). A. P. thanks Prof. F. J. Gießibl for his kind hospitality.

References

[1] Penzkofer, A. (1988) Passive Q-Switching and Mode-Locking for the Generation of Nanosecond to Femtosecond Pulses. *Applied Physics B*, **46**, 43-60. http://dx.doi.org/10.1007/BF00698653

[2] Penzkofer, A., von der Linde, D., Laubereau A. and Kaiser, W. (1972) The Intensity of Short Light Pulses Determined with Saturable Absorbers. *Optics Communications*, **4**, 377-379. http://dx.doi.org/10.1016/0030-4018(72)90082-X

[3] Blau, W., Reber, R. and Penzkofer, A. (1982) S_1-S_0 Relaxation Time of Saturable Absorber DDI. *Optics Communications*, **43**, 210-214. http://dx.doi.org/10.1016/0030-4018(82)90348-0

[4] Grönninger, G. and Penzkofer, A. (1984) Determination of Energy and Duration of Picoseconds Light Pulses by Bleaching of Dyes. *Optical and Quantum Electronics*, **16**, 225-233. http://dx.doi.org/10.1007/BF00619377

[5] Bansal, A.K., Holzer, W., Penzkofer, A. and Kley, E.B. (2008) Spectroscopic and Lasing Characterisation of a Dicarbazovinylene-MEH-Benzene Dye. *Optics Communications*, **281**, 3806-3819. http://dx.doi.org/10.1016/j.optcom.2008.03.032

[6] Luck, M., Mathes, T., Bruun, S., Fudim, R., Hagedorn, R., Nguyen, T.M.T., Kateriya, S., Kennis, J.T.M., Hildebrandt, P. and Hegemann, P. (2012) A Photochromic Histidine Kinase Rhodopsin (HKR1) that is Bimodally Switched by Ultraviolet and Blue Light. *Journal of Biological Chemistry*, **287**, 40083-40090. http://dx.doi.org/10.1016/j.optcom.2008.03.032

[7] Penzkofer, A., Luck, M., Mathes, T. and Hegemann, P. (2014) Bistable Retinal Schiff Base Photo-Dynamics of Histidine Kinase Rhodopsin HKR1 from *Chlamydomonas reinhardtii*. *Photochemistry and Photobiology*, in print. http://dx.doi.org/10.1111/php.12246

[8] Holzer, W., Gratz, H., Schmitt, T., Penzkofer, A., Costela, A., García-Moreno, I., Sastre, R. and Duarte, F.J. (2000) Photo-Physical Characterization of Rhodamine 6G in a 2-Hydroxyethyl-Methacrylate Methyl-Methacrylate Copolymer. *Chemical Physics*, **256**, 125-136. http://dx.doi.org/10.1016/S0301-0104(00)00101-4

[9] Valeur, B. (2002) Molecular Fluorescence. Principles and Applications, Wiley-VCH, Weinheim, Germany.

[10] Hercher, M. (1967) An Analysis of Saturable Absorbers. *Applied Optics*, **6**, 947-954. http://dx.doi.org/10.1364/AO.6.000947

[11] Bentivegna, F., Canva, M., Georges, P., Brun, A., Chaput, F., Malier, L. and Boilot, J.-P. (1993) Reverse Saturable Absorption in Solid Xerogel Matrices. *Applied Physics Letters*, **62**, 1721-1723. http://dx.doi.org/10.1063/1.109585

[12] Fischer, H., Polikarpov, I. and Craievich, A. (2004) Average Protein Density is a Molecular-Weight-Dependent Function. *Protein Science*, **13**, 2825-2828. http://dx.doi.org/10.1110/ps.04688204

[13] Penzkofer, A., Falkenstein, W. and Kaiser, W. (1976) Vibronic Relaxation in the S_1-State of Rhodamine Dye Solutions. *Chemical Physics Letters*, **44**, 82-87. http://dx.doi.org/10.1016/0009-2614(76)80414-9

[14] Graf, F. and Penzkofer, A. (1985) S_n-State Lifetime Determination of Dyes. *Optical and Quantum Electronics*, **17**, 53-68. http://dx.doi.org/10.1007/BF00619994